A comparative study of multiple scattering calculations implemented in general–purpose Monte Carlo and selected Ion Beam Analysis codes

E. G. Androulakaki[1], M. Kokkoris[1,a], M. Mayer[2], E. Mitsi[1], N. Patronis[3], E. Vagena[3,4]

[1] *Department of Physics, National Technical University of Athens, Zografou Campus, 15780 Athens, Greece*

[2] *Max–Planck–Institut für Plasmaphysik, Boltzmannstr. 2, D–85748 Garching Germany*

[3] *Department of Physics, University of Ioannina, 45110 Ioannina, Greece*

[4] *Institute of Nuclear and Particle Physics, NCSR "Demokritos", Aghia Paraskeui 153 10, Greece*

Abstract

In the present work extensive multiple scattering (i.e. angular straggling) calculations were performed, implementing general–purpose Monte Carlo codes (GEANT4, MCNP6.1, FLUKA, PHITS) and selected, dedicated ion beam analysis programs (such as SRIM2013 and SIMNRA7.03), using 158.6 MeV protons impinging on a variety of thin or semi–thick, pure, single–element targets, such as carbon, aluminum, copper, tin, lead, beryllium and zinc, which are typically used as shielding materials or components in complex devices, in order to investigate all the occurring differences and similarities with respect to the experimental results obtained in the classic work of Gottschalk et al. [1]. Polystyrene was the only compound target to be examined, since it is a plastic commonly used in various applications. The obtained results are presented in

[a] Corresponding author, email: kokkoris@central.ntua.gr

graphical form, as ratios to the available experimental data from [1] for various target thicknesses and are subsequently discussed and analyzed.

Keywords: Monte Carlo codes; GEANT4, FLUKA, PHITS, MCNP, Multiple Scattering; Angular Straggling; SRIM2013; SIMNRA

PACS No: 11.80.La; 24.10.Lx; 87.55.K-; 82.80.Yc

1. Introduction

The multiple scattering calculations, inherently implemented in all widely used, general–purpose Monte Carlo (MC) codes, play a critical role in the determination of any expected dose yield and are directly related to volume damage effects. Small changes in multiple scattering (lateral, i.e. angular straggling), and therefore in the corresponding particle trajectories, can lead to significant changes in the affected target or detector irradiated areas. This effect may be critical in the ion beam modification of materials, as well as, in beam transport in accelerators, fusion research and hadron therapy applications. Moreover, to the authors' best knowledge, except for a recent comprehensive study focused on GEANT4 [2], a corresponding comparison of all the main Monte Carlo codes, along with selected ion beam analysis (IBA) ones, such as SRIM2013 and SIMNRA v.7.03, with high–accuracy experimental data has never been thoroughly carried out in the past.

Thus, the aim of the present work is to examine the differences in the multiple scattering calculations between GEANT4 v.10.5.p01 [3], FLUKA v.2011.2x.6 [4], MCNP6.1 [5], PHITS v.2.88 [6], SRIM2013 [7] and SIMNRA v.7.03 [8], using 158.6 MeV protons impinging on a variety of thin, semi–thick, or thick, pure, single–element targets, such as carbon, aluminum, copper, tin, lead, beryllium and zinc, which are typically used as shielding materials or components in complex devices, in order to investigate all the occurring differences and similarities with respect to the experimental results obtained in

the classic work of Gottschalk et al. [1], published almost 30 years ago. In all cases the default models were used, as implemented in the corresponding MC codes. Polystyrene was the only compound target to be examined, since it is a plastic material commonly employed in various technological and commercial applications. However, since the present work was limited to only one ion species and bombarding energy, the subject requires further investigation over a broad energy range and for a variety of impinging ions. Undoubtedly, the main constraint for the expansion of such a study is the relative lack of high–quality, benchmarked experimental data, for a variety of beam–target combinations and energies, despite the considerable recent efforts, evident in literature, e.g. [9–10]. The final values are presented in graphical form and the observed similarities and discrepancies with the experimental results are discussed and analyzed. Nevertheless, as previously mentioned, due to the absence of a comprehensive experimental review with suggested benchmarked datasets over a broad energy range, and for a large variety of ion beam–target combinations, the final assessment of the obtained results relies on the user. It should also be stressed here that, in compliance with the FLUKA user license, any validation of the Monte Carlo codes used is beyond the scope of this work.

The basic theoretical work on small angle multiple scattering of ions in matter was carried out since the 1920's by pioneers like Bothe [11], followed in the 40's and 50's by Molière [12], Meyer [13] and Bethe [14], while Scott [15] summarized the state of knowledge in this field in 1963 and later, a milestone contribution was brought in by Sigmund and coworkers in a series of papers [16–18], which included tabulated spatial angular distributions, widely used ever since in ion beam analysis, following, among others, the works of Goudsmit and Saunderson [19] and Lindhard and Nielsen [20]. The theory behind multiple scattering calculations has been thoroughly analyzed in [21] and

has been summarized in [22]. Briefly stated, it is based on the following general assumptions: (1) the scattering centers are randomly distributed and the containing medium is homogeneous, (2) the ion follows a series of binary collisions which present azimuthal symmetry, (3) the energy losses can in principle be added separately, (4) the scattering angles are small and (5) the multiple scattering on electrons can also be included as an additive term. A detailed presentation of all the different theoretical approaches can be found elsewhere (e.g. [21–22]), however, it is important to note that despite the great differences between the implemented ion–atom scattering cross sections (e.g via the use of Molière, ZBL, Thomas–Fermi, or Lenz–Jensen screening potentials), all model predictions seem to be in good agreement with one another for targets of medium thickness, that is, following a relatively large number of successive collisions of the ion inside the target. Strong deviations are in principle expected only in the tails of the calculated distributions (e.g. for ultra–thin targets).

2. Calculation details

As stated in the previous section, there is a large variety of adopted approaches for the multiple scattering calculations among the existing codes and the corresponding theoretical literature is very rich, therefore each studied case presented unique characteristics. More specifically:

(a) GEANT4, v.10.5.p01 incorporates two basic models concerning multiple scattering [23]. The so-called Urban model [24] was the default one till the version 10.1. It is based on Lewis theory and has separate parameterizations [25] of the central part of the scattering angle and its tail (due to large–angle scattering events). Various data are used for the tuning of the function

describing the tail of the scattering function and it is applicable to any particle type, at any energy. The second model is the newer WentzelVI one, employing the Wentzel scattering function [26] for small scattering angles, namely below 0.2 radian, while higher scattering angles are calculated using the single Coulomb scattering model, as implemented in GEANT4 version 10.2. In the present work the default multiple scattering option was adopted as implemented in the corresponding version of GEANT4. Moreover, concerning the choice of electromagnetic libraries, recent results indicate that for protons the most suitable option is the G4EmStandardPhysics_option4 (Opt4) one and for this selection the step limit function was modified to 0.02–0.01 μm in order to improve the accuracy of the calculations [2].

(b) FLUKA implements the Molière theory [12], which makes use of the small angle approximation to derive a multiple scattering distribution which is valid, provided that the number of elementary scatterings is large enough (>20), as mentioned in the previous section. The underlying single scattering cross section is the Rutherford one corrected for screening. The model is in principle able to describe the distribution function of any single physical quantity of interest (e.g. polar scattering angle, projected angle, position angles and lateral displacement), even though it does not provide any means for computing the joint distribution of two or more of these quantities [27]. The model is composed of two successive parts, namely the path length correction algorithm (in order to achieve the greatest possible step length insensitivity) and the correlation algorithm for the various angles involved in each step simulation.

(c) PHITS uses the code ATIMA, developed at GSI (https://web–docs.gsi.de/~weick/atima/ also implemented in LISE++ [28]), which calculates the stopping power and the angular straggling of protons and heavy ions in matter for energies ranging from 1 keV/u to 450 GeV/u. It is largely based [29] on the treatment by Marion and Zimmerman [30], derived from Molière's theory. The code distinguishes the multiple scattering treatment on the basis of the Born parameter which is described by the following formula:

$$\alpha_B = \frac{Z_1 Z_2}{137\beta}, with\ \beta = \frac{u}{c}$$

When α_B<1, a condition which is valid for medium energy protons implemented in the present work on any target, the Molière theory can give reliable quantitative results.

(d) In MCNP6.1 the angular straggling is again modeled according to a modified version of the multiple scattering theory developed by Molière. Users have the option of selecting one of several relevant models. The first two models, FNAL1 and FNAL2 (default), are referred to as the Fermi National Lab models or sometimes as the Striganov Models [31] in the corresponding manual of the code, while the third model is a simpler Gaussian approximation to the angular straggling distribution. Using the first two options the angular scattering component of an impinging particle is calculated in conjunction with energy straggling, providing a model closer in theory to a single–event method.

(e) SIMNRA is an analytical simulation program for RBS, ERDA, NRA and MEIS energy spectra with MeV ions [8, 32]. It calculates multiple scattering using an independent implementation of the theory presented by Szilágyi et al. [33] and

Amsel et al. [22], whose work expanded the theory developed by Sigmund and Winterbon [16] for multi–elemental targets including stopping, by subdividing such a target into thin mono–elemental slabs with the energy loss in each slab being sufficiently small, so that the Sigmund–Winterbon theory can be applied for each slab. They also provided easy–to–use fit formulas for the universal angular spread function from [16]. The results of Szilágyi et al. [33] were subsequently implemented in the pioneer DEPTH code (https://www.kfki.hu/~ionhp/doc/prog/depth.htm). The DEPTH code and SIMNRA were compared in [34] and demonstrated a very good agreement. For this work the range of tabulated stopping powers in SIMNRA was increased to 200 MeV, while SRIM2013 values [7] were used for all the calculations.

(f) SRIM2013 is (unlike all the previous ones) a binary collision MC code and is generally acknowledged as being the standard program for low–energy applications regarding stopping power, energy and angular straggling calculations of heavy ions (Z>1) in matter. Concerning multiple scattering, it implements the Lindhard–Nielsen approach, but using the ZBL (universal) interatomic potential and screening function instead of the Thomas–Fermi one. The results are stored in tabular form as ASCII files and contain the directional cosines of the ion trajectories at the exit of the target.

3. Geometry and experimental details

As mentioned above, the highly detailed and reference experimental dataset from Gottschalk et al. [1], which contains almost 20 years of multiple scattering measurements at the Harvard Cyclotron Laboratory, was selected for comparison with the MC and IBA

code results. In this work, monoenergetic protons at 158.6 MeV impinged on a variety of materials. For comparison purposes, only data from carbon, aluminum, copper, tin, lead, beryllium, zinc and polystyrene were implemented in the present work, covering a wide range of normalized target thicknesses – defined in [1] as the target thickness divided by the proton range – varying from 0.002 to ~1. In the experiment, at z_D=100 cm from the target surface, as shown in figure 1a, the beam profile was measured using a diode and for each case, the position x_i was converted to a corresponding angle θ_i following the relation:

$$\theta_i = arctan\left(\frac{x_i}{z_E}\right)$$

A small correction to the source to detector distance has to be applied during data analysis, concerning the determination of the effective origin (i.e. initial point) of the multiple scattered protons coming from a target, which subsequently leads to the determination of the effective distance z_E with respect to z_D. For small target thicknesses the effective origin tends to correspond to the middle of the target, as shown in figure 1a, but for larger ones approaches the exit face of the target, as shown in figure 1b. Since the effective origin as a fraction of target thickness is a nearly universal function of the normalized target thickness, the applied minor correction was based on a careful digitization of figure 5b from [1].

For all the implemented MC codes the same exact procedure was followed, with the only simplification being the adoption of a pencil beam (i.e. ignoring the finite experimental opening of the collimator and anti–scatterer defining slits in [1]). In each case 10^7–10^8 events were generated in order to acquire sufficient statistics over at least 100 bins in the scoring surface. Since the elastic scattering is φ–invariant (azimuthal symmetry), the resulting r_i distributions (i.e. distances from the zero, 'non–divergent' point on the detector

surface) were fitted with a Gaussian type function using standard χ^2 minimization, as in [2]. Large single angle scattering events (constituting the long tails of the distribution) had a negligible effect in the fitting procedure, while nuclear contributions were fully suppressed in all MC codes (data points of less than 5% of the maximum were not considered for fitting, thus excluding contributions of large single angle scattering). The uncertainties in the thus obtained FWHM values did not exceed 1-2% in all cases and the reproducibility of the results, as tested for various numbers of generated events (but always exceeding 10^7) in selected target materials and thicknesses was better than 1%.

SIMNRA, on the other hand, calculates the FWHM of the multiple-scattering angular spread distribution analytically, based on [33, eq. 46]. The FWHM can be monitored with the program *Viewnra,* which is included in the SIMNRA distribution and can be used to investigate all internal calculations. The only modification of the corresponding code, as mentioned in the previous section, concerned the extension of the stopping power tables for protons from 50 MeV to 200 MeV, in order to comply with the requirements of Gottschalk's work for comparison purposes.

SRIM2013 was the only code to be separately treated, due to the fact that the final position of the recorded events referred to the back side of the targets (beam exit face), determined by the corresponding directional cosines. In order to render such results comparable to the ones obtained with the analytical MC codes, MCNP6.1 was tuned to generate the same distributions, imitating the SRIM2013 simplified geometry, so the corresponding Monte Carlo calculation was repeated in this case for aluminum, copper, polystyrene, beryllium and lead, without applying any type of subsequent analytical corrections.

4. Results and discussion

The obtained results from all the MC codes and SIMNRA are presented in figs. 2a–h and include all the examined materials and tested thicknesses. The simulated values are plotted in the form of ratios to the experimental values from [1] versus each target thickness (in g/cm^2). In the figures the experimental errors from Gottshalk's work as well as the corresponding ones from the codes (practically almost equivalent with the ones determined for the ratios) can also be depicted, along with the corresponding thickness/range values from table 3 of [1]. Taking into account that the obtained experimental results from [1] presented deviations from Molière theory ranging from 0.1 to 18.8% for the investigated targets in the present work, it was deemed reasonable to distinctly mark a ±20% interval in the graphs, as an appropriate, indicative confidence level for the corresponding deviations.

As shown in figures 2a–h, the vast majority of the simulated results fall within this confidence level range. This is quite encouraging, taking into account the profound implications of angular straggling in dosimetry, beam transport and fusion applications. In general, for all the targets, GEANT4, (max: 1.21, min: 0.90, mean: 1.04) and FLUKA (max: 1.34, min: 0.79, mean: 1.00) values seem to be – on average – closer to the experimental results from [1]. For GEANT4 this behavior has also been demonstrated in detail in [2] and the results from the present work are similar. MCNP (max: 1.26, min: 0.80, mean: 1.11) and SIMNRA (max: 1.41, min: 0.79, mean: 1.08) values tend to be slightly overestimated, while PHITS ones (max: 1.19, min: 0.77, mean: 0.94) relatively underestimated. It should be noted though, that since SIMNRA is not a MC code, these calculations are carried out in only a fraction of the computing time required by the other codes, without any significant loss in accuracy. Moreover, the underlying Sigmund–Winterbon theory [16] was initially developed for reduced thicknesses τ below 2000 (i.e.

below 10–50 μm), requiring a substantial extrapolation for the present case of 158.6 MeV protons with much larger penetration depths. In general, the greatest deviations appear at very small and very large target thicknesses. For the former case, the theory utilized by many codes may need further tuning, or is not completely valid (since the corresponding number of expected collisions is consequently small), while for the latter, the entanglement of the multiple scattering effect with the energy straggling one may be the cause of the observed discrepancies.

A slight Z–dependence of the discrepancies for medium target thicknesses can also be observed, since there exists a relative increase of the ratios for heavier materials (e.g. comparing the corresponding values for beryllium, carbon, polystyrene and aluminum with the ones for tin and lead). In general, no other systematic trends with respect to the experimental data were observed. As an example, the corresponding behavior of SIMNRA is depicted in fig. 3, where the deviations of the theoretical solid curves from the experimental points (for all figures taken from [1], table 3, θ_M values) for the targets under consideration become significant only at large target thicknesses.

For the specific case of SRIM2013, where directional cosines at the beam exit face have been implemented, the ratios of the obtained mean angular values using MCNP6.1 with respect to the SRIM ones (for ~30000 generated events) are depicted in figures 4a–e for the cases of aluminum, copper, polystyrene, beryllium and lead respectively. The average values of the ratios for all the calculated points per each target are indicated in the graphs with a dotted line. SRIM values tend to systematically overestimate the MCNP ones for all the examined targets (average ratios are always below unity, as follows, Al : 0.91±0.07, Cu : 0.87±0.07, Polystyrene : 0.92±0.07, Be : 0.93±0.13, Pb : 0.88±0.08). The existence of a few significant deviations from the average values may be partly attributed

to stopping power differences, especially for small target thicknesses. A detailed review on this problem has recently been presented in literature [35]. As a whole, although SRIM results are not directly comparable with the experimental ones from [1], taking into account that, when the full geometry of the problem is implemented in MCNP, the latter yields slightly higher values than the ones obtained with the other Monte Carlo codes, it is reasonable to assume that with SRIM2013 the observed discrepancies would have been accordingly higher.

5. Conclusions

In the present work a comparative study of multiple scattering calculations from widely used MC and selected IBA codes with experimental data from the pioneer work of Gottschalk et al. [1] has been presented for the first time. There is a general, encouraging overall agreement (within ~20% in the vast majority of the cases) between the obtained results. This satisfactory result is critical for all ion beam irradiation applications.

It is important to stress here, however, that since there do not exist benchmarked experimental multiple scattering datasets over a considerably broad energy range and for a large variety of ion beam–target combinations, the final assessment of the obtained results relies on the users, who should constantly exploit the literature, especially for new experiments concerning heavy ion projectiles at high energies (namely for $\alpha_B >> 1$). It is also evident from the present study, that despite the tremendous progress achieved so far concerning scientific coding, a coordinated effort on the experimental front is still required before a complete convergence of the codes in the problem of multiple scattering values is reached. New, validated experimental data would consequently lead to the appropriate

fine–tuning of the corresponding model–dependent parameters implemented in each program.

Acknowledgement

The authors gratefully acknowledge the financial and scientific support from the European Space Agency (Contract No. 4000112863/14/NL/HB).

References

[1] B. Gottschalk, A. Koehler, R. Schneider, J. Sisterson, M. Wagner, *Nucl. Instr. and Meth.* **B74** (4) (1993), p. 467–490.

[2] H. Fuchs, S. Vatnitsky, M. Stock, D. Georg, L. Grevillot, *Nucl. Instr. and Meth.* **B410** (2017), p. 122–126.

[3] Geant4 Collaboration, Geant4 Release 10.5, Users Manual, 2017, and J. Allison et al., *Nucl. Instr. and Meth.* **A835** (2016), p. 186–225.

[4] Fluka: A multi–particle transport code, CERN–2005–010, 2005.

[5] MCNP6 Users Manual – Code Version 6.1, LA–CP–13–00634 (2013).

[6] T. Sato, K. Niita, Y. Iwamoto, S. Hashimoto, T. Ogawa, T. Furuta, S. Abe, T. Kai, N. Matsuda, K. Okumura, T. Kai, H. Iwase and L. Sihver, *EPJ Web of Conferences* **153**, 06008 (2017).

[7] J. F. Ziegler, J. P. Biersack, M. D. Ziegler, *'The Stopping and Range of Ions in Matter'*, Lulu Press Co, Morrisville, NC, 27560 USA, (2015).

[8] M. Mayer, *Nucl. Instr. and Meth.* **B332** (2014) 176.

[9] W. Scandale et al., *Nucl. Instr. and Meth.* **B402** (2017), p.291–295.

[10] P. Pan et al., *Nucl. Instr. and Meth.* **B450** (2019), p.332–336.

[11] W. Bothe, *Z. Phys*. **5** (1921), p. 63.

[12] G. Molière, *Z. Naturforschung*. **A3** (1948), p. 78.

[13] L. Meyer, *Phys. Stat. Sol. (b)* **44** (1971), p. 253.

[14] H. A. Bethe, *Phys. Rev*. **89** (1953), p. 1256–1266.

[15] W.T. Scott, *Rev. Mod. Phys.* **35** (2) (1963), p. 231.

[16] P. Sigmund, K.B. Winterbon, *Nucl. Instr. and Meth.* **119** (1974), p. 541.

[17] A.D. Marwick, P. Sigmund, *Nucl. Instr. and Meth.* **126** (1975), p. 317.

[18] P. Sigmund, J. Heinemeier, F. Besenbacher, P. Hvelplund, H. Knudsen, *Nucl. Instr. and Meth.* **150** (1978), p. 221.

[19] S. Goudsmit, J. L. Saunderson, *Phys. Rev.* **57** (1940) 24.

[20] J. Lindhard, V. Nielsen, M. Scharff, *Math. Phys. Medd. Vid. Selsk.* **38** (1968).

[21] P. Sigmund, 'Particle penetration and radiation effects' Vol. 2, Springer Series in Solid–State Sciences **179** (2014).

[22] G. Amsel, G. Battistig, and A. L'Hoir, *Nucl. Instr. and Meth.* **B201** (2003), p. 325–388.

[23] V. N. Ivanchenko, O. Kadri, M. Maire, and L. Urban, *J. of Physics: Conference Series* **219** (2010) 032045.

[24] L. Urban, 'A multiple scattering model in Geant4', *Preprint CERN–OPEN–2006–077* (2006).

[25] F. Salvat, A. Jablonski and C. J. Powell, *Comp. Phys. Comm.* **165** (2005), p. 157.

[26] G. Wentzel, *Zeitschrift für Phys.* **43 (1–2)** (1927), p. 1–8.

[27] A. Ferrari, P. R. Sala, R. Guaraldi and F. Padoani, *Nucl. Instr. and Meth.* **B71** (1992), p. 412–426.

[28] O. Tarasov, D. Bazin, M. Lewitowicz, O. Sorlin, *Nucl. Phys.* **A701** (2002), p. 661c–665c.

[29] R. Anne, J. Herault, R. Bimbot, H. Gauvin, G. Bastin, F. Hubert, *Nucl. Instr. and Meth.* **B34** (1988), p. 295–308.

[30] J. B. Marion and F. C. Young, '*Nuclear Reaction Analysis', Graphs and Tables* (North–Holland, Amsterdam, 1968).

[31] S. I. Striganov, *Radiat Prot Dosim*. **116(1)** (2005), p.293–296.

[32] M. Mayer, 'SIMNRA User's Guide', *Tech. Rep. IPP 9/113*, Max–Planck–Institut für Plasmaphysik, Garching (1997).

[33] E. Szilágyi, F. Pászti, and G. Amsel, *Nucl. Instr. and Meth.* **B100** (1995), p. 103.

[34] M. Mayer, K. Arstila, K. Nordlund, E. Edelmann, and J. Keinonen, *Nucl. Instr. and Meth.* **B249** (2006), p. 823.

[35] E. Vagena, E. G. Androulakaki, M. Kokkoris, N. Patronis and M. E. Stamati, *Nucl. Instr. and Meth.* **B467** (2020), p. 44.

Figure captions

Figure 1a–b. (a) Simplified schematic diagram of the experimental setup from [1] which was implemented in the Monte Carlo simulations and (b) Demonstration of the required small correction for the effective origin of multiply scattered protons in a thick target.

Figure 2a–h. Ratio of the simulated results obtained with all the Monte Carlo codes and SIMNRA with respect to the corresponding experimental ones from the pioneer work of Gottschalk et al. [1], versus each target thickness (expressed in g/cm^2) in the case of : (a)

Aluminum (b) Copper (c) Carbon (d) Polystyrene (e) Tin (f) Zinc (g) Beryllium and (h) Lead. The corresponding errors are also shown, while the top horizontal axis denotes the thickness over total range ratio according to [1].

Figure 3. Experimentally determined Θ values (points, in mrad), corresponding to the Θ_M column in table 3 from [1], along with the SIMNRA theoretical predictions (shown as solid lines), as a function of target thickness (in g/cm^2) for various materials. The corresponding errors have been omitted from the graph for reasons of clarity.

Figure 4a–e. Ratio of the MCNP6.1 results with respect to the SRIM2013 ones using directional cosines in the beam exit face versus each target thickness (expressed in g/cm^2) in the case of : (a) Aluminum (b) Copper (c) Polystyrene (d) Beryllium and (e) Lead. The average value of this ratio for all the calculated points is indicated in the graphs with a dotted line. The corresponding errors are also shown, while the top horizontal axis denotes the thickness over total range ratio according to [1].

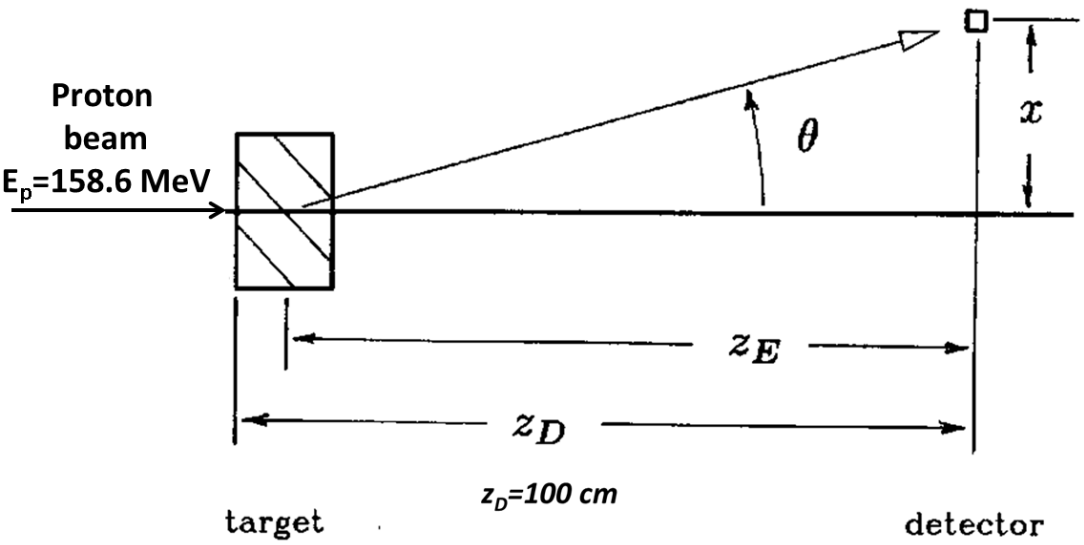

Figure 1a

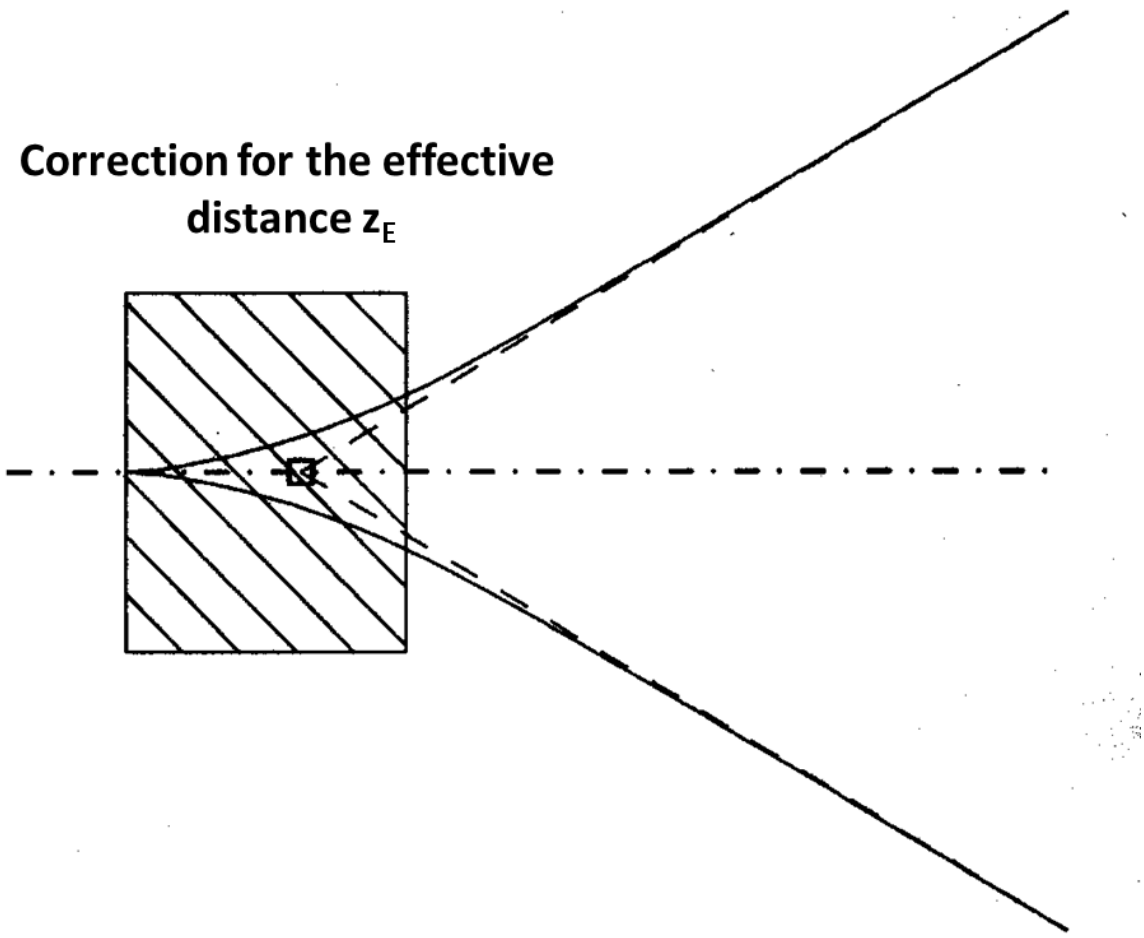

Figure 1b

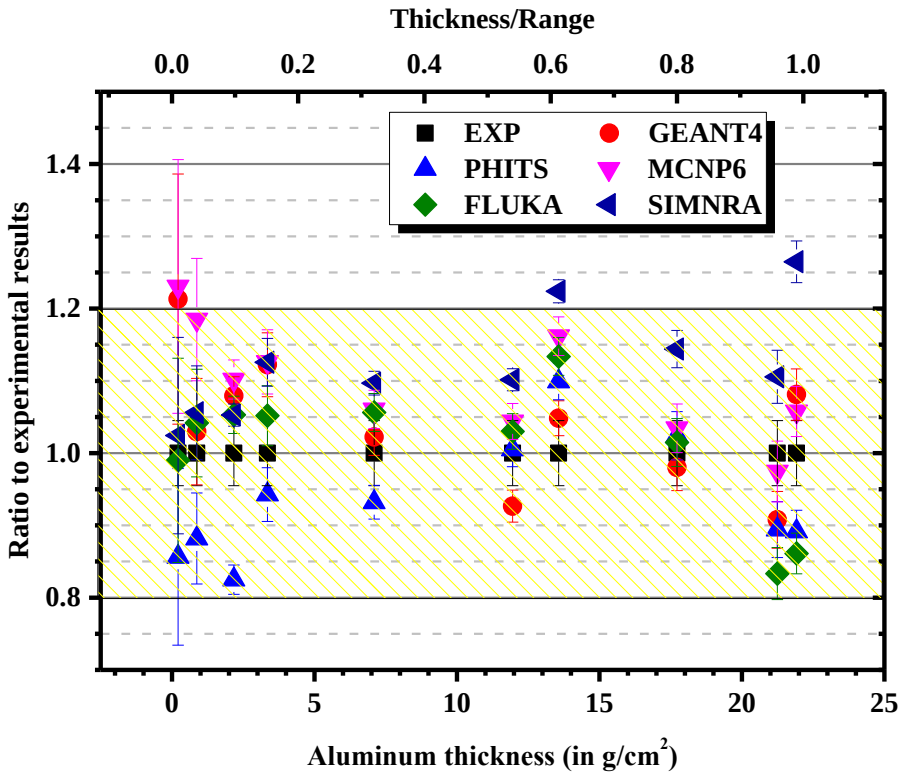
Thickness/Range
0.0
0.2
0.4
0.6
0.8
1.0
EXP
PHITS
FLUKA
GEANT4
MCNP6
SIMNRA
Ratio to experimental results
1.4
1.2
1.0
0.8
0
5
10
15
20
25
Aluminum thickness (in g/cm^2)

Figure 2a

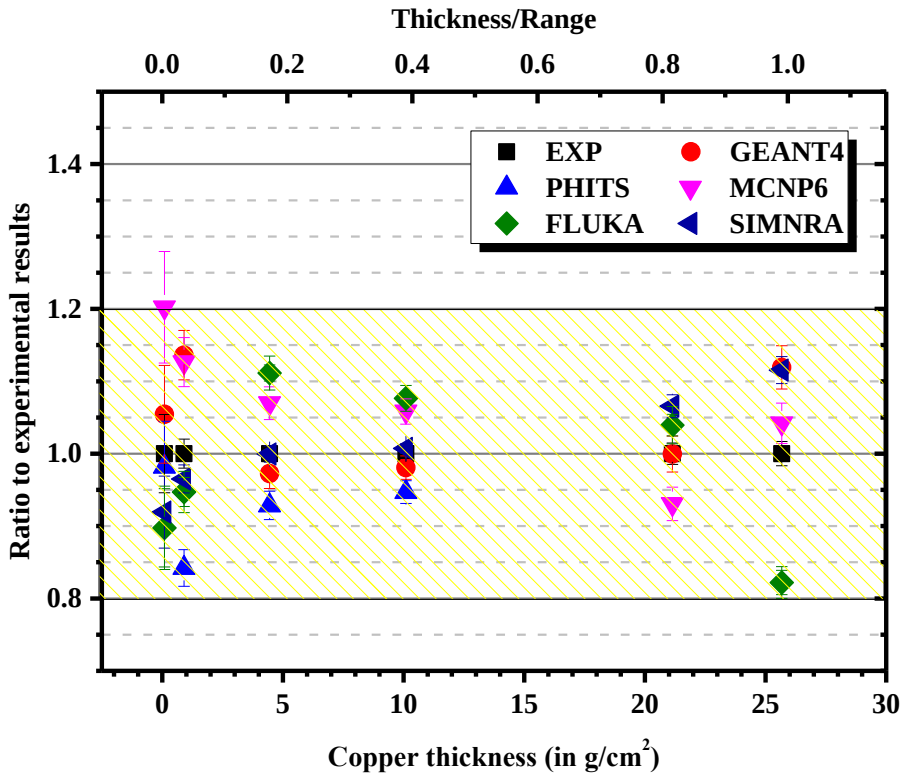
Thickness/Range
0.0
0.2
0.4
0.6
0.8
1.0
EXP
GEANT4
PHITS
MCNP6
FLUKA
SIMNRA
Ratio to experimental results
1.4
1.2
1.0
0.8
0
5
10
15
20
25
30
Copper thickness (in g/cm^2)

Figure 2b

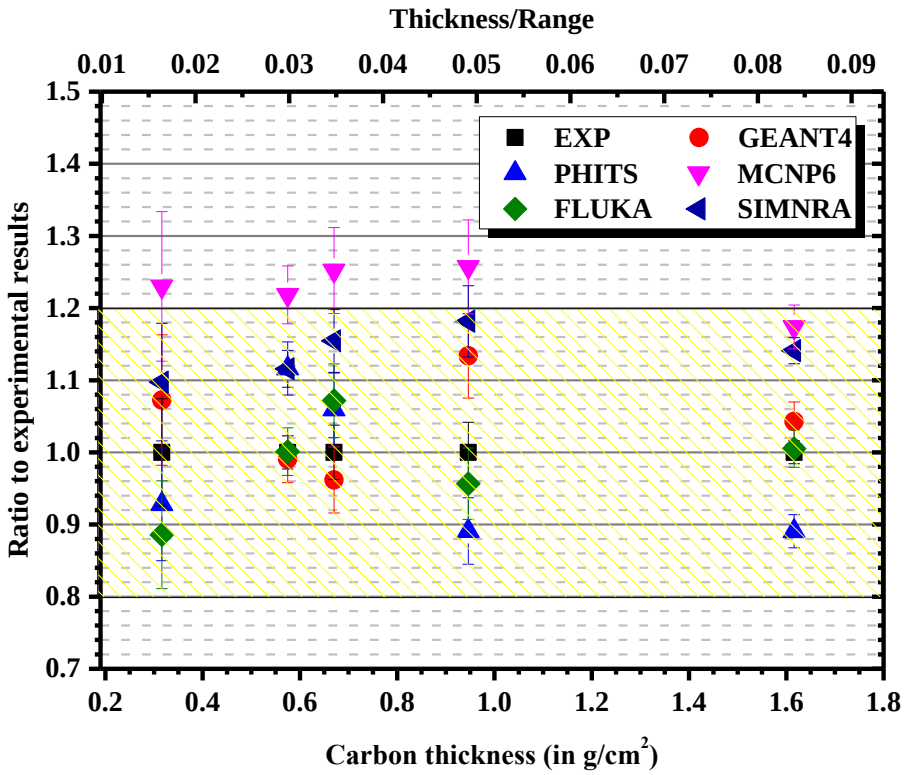
Thickness/Range
0.01
0.02
0.03
0.04
0.05
0.06
0.07
0.08
0.09
1.5
1.4
1.3
1.2
1.1
1.0
0.9
0.8
0.7
Ratio to experimental results
EXP
GEANT4
PHITS
MCNP6
FLUKA
SIMNRA
0.2
0.4
0.6
0.8
1.0
1.2
1.4
1.6
1.8
Carbon thickness (in g/cm2)

Figure 2c

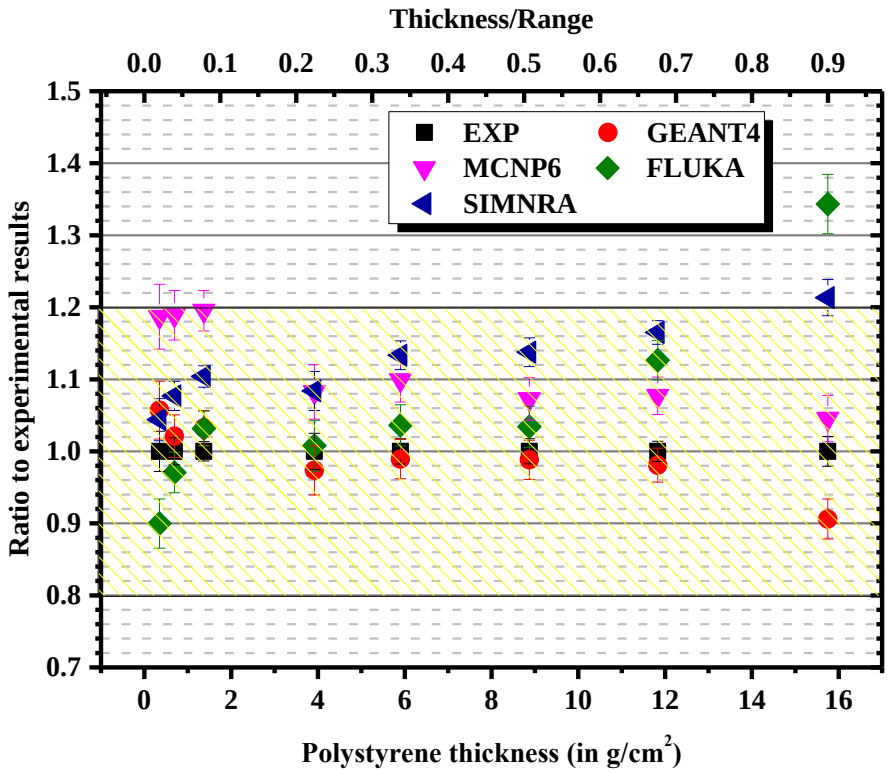
Thickness/Range
0.0
0.1
0.2
0.3
0.4
0.5
0.6
0.7
0.8
0.9
1.5
1.4
1.3
1.2
1.1
1.0
0.9
0.8
0.7
Ratio to experimental results
EXP
GEANT4
MCNP6
FLUKA
SIMNRA
0
2
4
6
8
10
12
14
16
Polystyrene thickness (in g/cm2)

Figure 2d

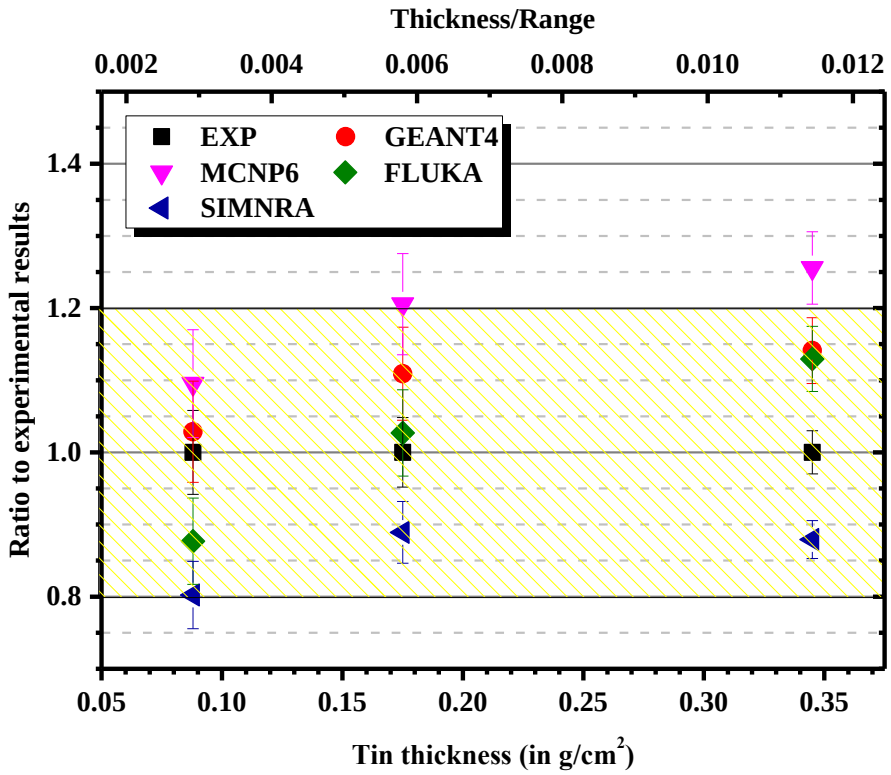
Thickness/Range
0.002
0.004
0.006
0.008
0.010
0.012
EXP
GEANT4
MCNP6
FLUKA
SIMNRA
Ratio to experimental results
1.4
1.2
1.0
0.8
0.05
0.10
0.15
0.20
0.25
0.30
0.35
Tin thickness (in g/cm^2)

Figure 2e

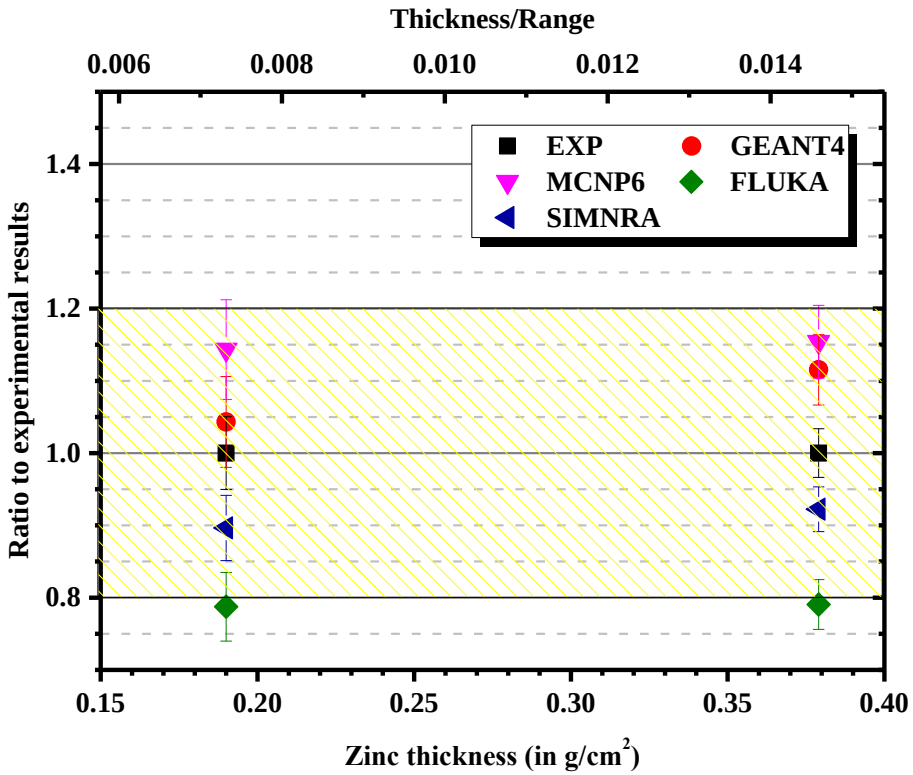
Thickness/Range
0.006
0.008
0.010
0.012
0.014
EXP
GEANT4
MCNP6
FLUKA
SIMNRA
Ratio to experimental results
1.4
1.2
1.0
0.8
0.15
0.20
0.25
0.30
0.35
0.40
Zinc thickness (in g/cm^2)

Figure 2f

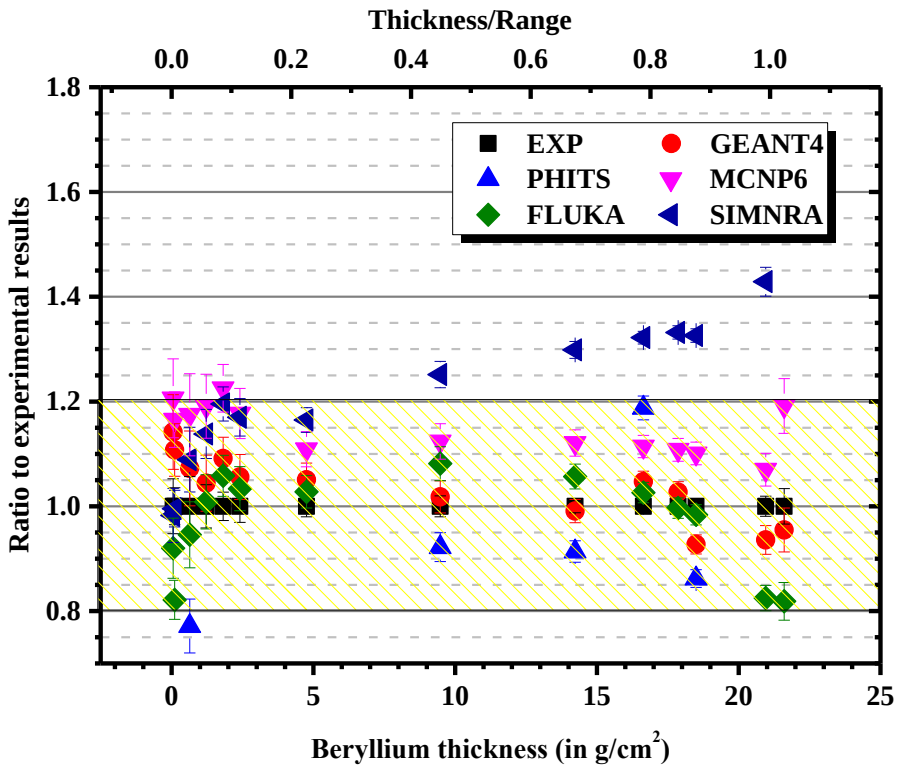
Thickness/Range
0.0
0.2
0.4
0.6
0.8
1.0
1.8
1.6
1.4
1.2
1.0
0.8
Ratio to experimental results
EXP
GEANT4
PHITS
MCNP6
FLUKA
SIMNRA
0
5
10
15
20
25
Beryllium thickness (in g/cm^2)

Figure 2g

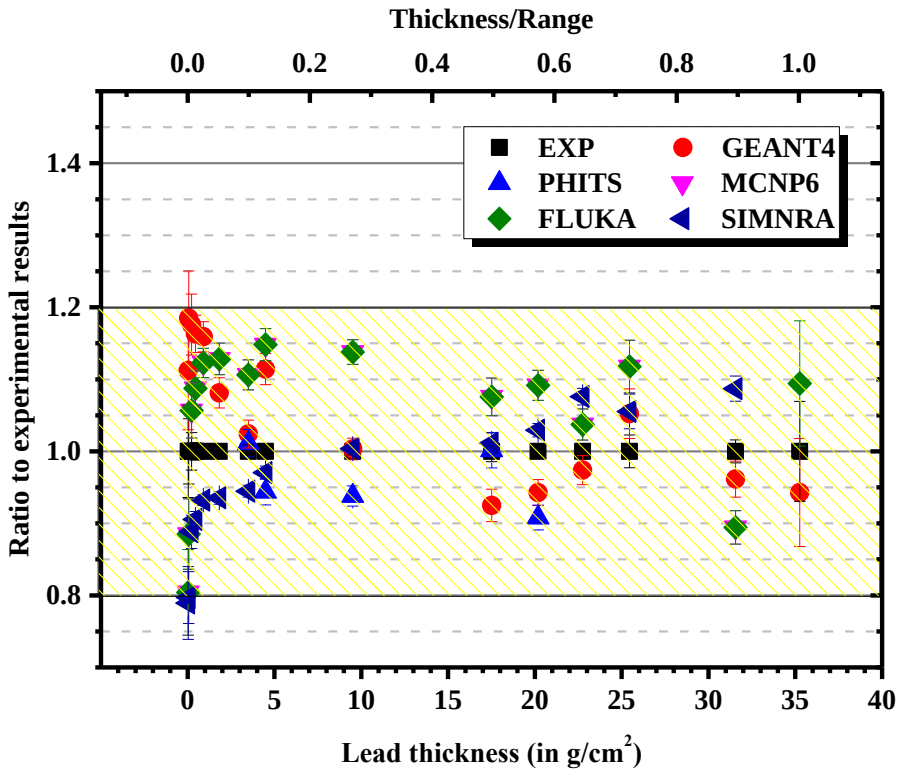
Thickness/Range
0.0
0.2
0.4
0.6
0.8
1.0
EXP
GEANT4
PHITS
MCNP6
FLUKA
SIMNRA
Ratio to experimental results
1.4
1.2
1.0
0.8
0
5
10
15
20
25
30
35
40
Lead thickness (in g/cm^2)

Figure 2h

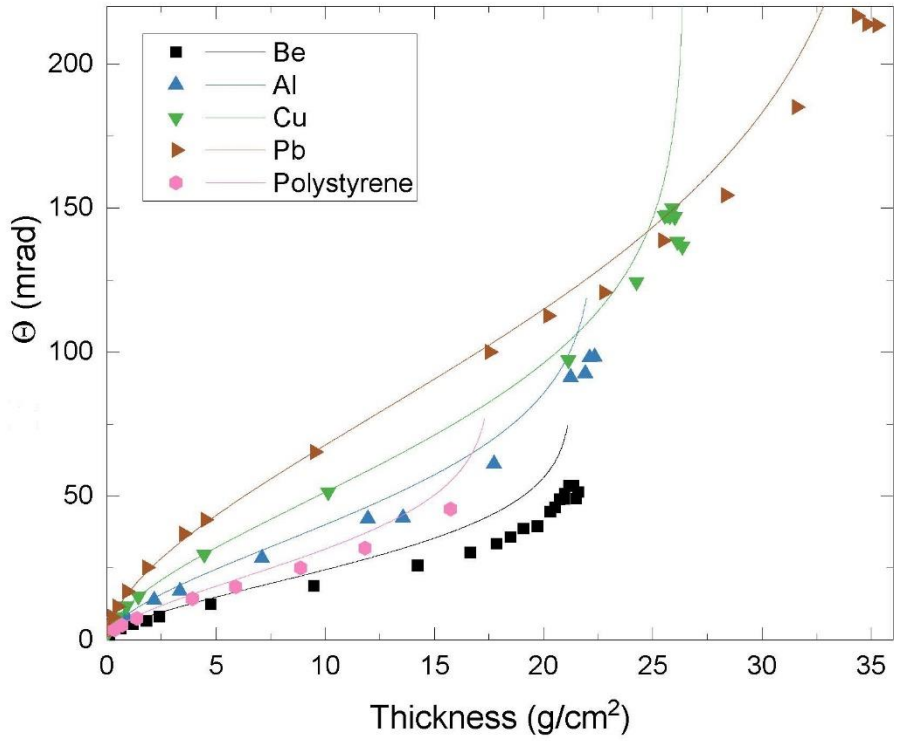
Be
Al
Cu
Pb
Polystyrene
Θ (mrad)
Thickness (g/cm²)
0
50
100
150
200
0
5
10
15
20
25
30
35

Figure 3

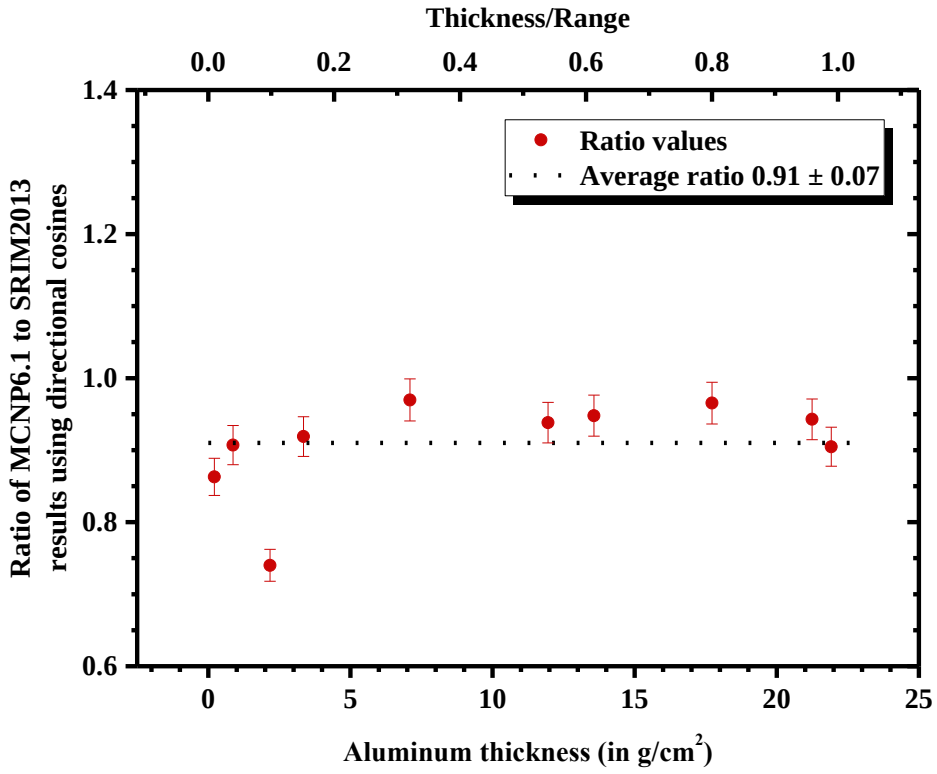
Thickness/Range
0.0
0.2
0.4
0.6
0.8
1.0
1.4
1.2
1.0
0.8
0.6
Ratio of MCNP6.1 to SRIM2013 results using directional cosines
Ratio values
Average ratio 0.91 ± 0.07
0
5
10
15
20
25
Aluminum thickness (in g/cm^2)

Figure 4a

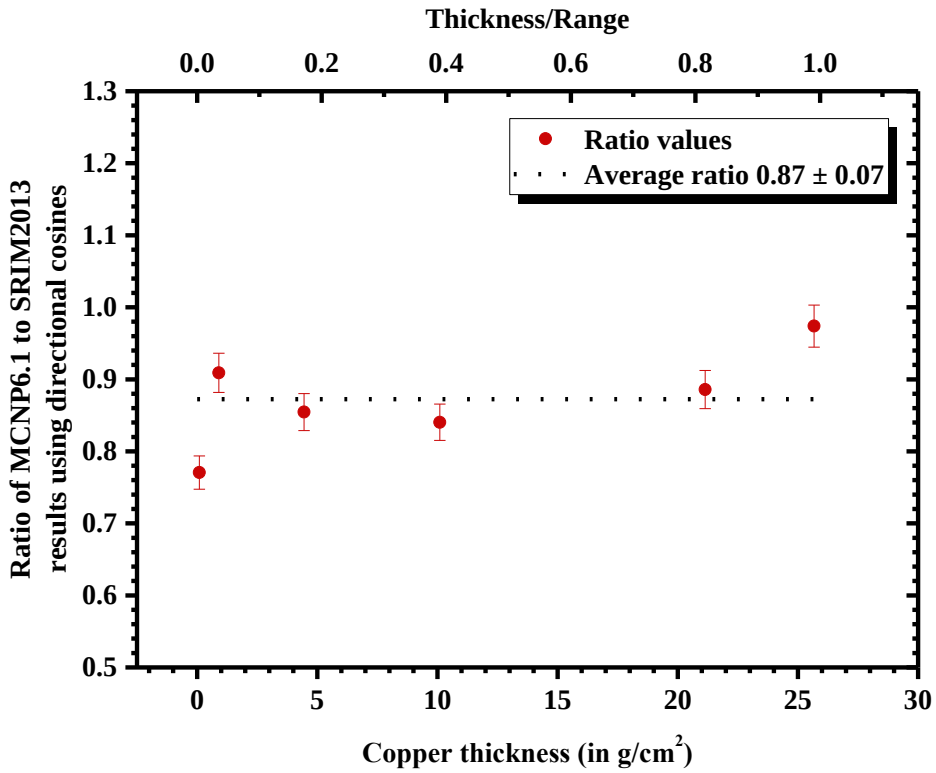
Thickness/Range
0.0
0.2
0.4
0.6
0.8
1.0
1.3
1.2
1.1
1.0
0.9
0.8
0.7
0.6
0.5
Ratio of MCNP6.1 to SRIM2013 results using directional cosines
Ratio values
Average ratio 0.87 ± 0.07
0
5
10
15
20
25
30
Copper thickness (in g/cm2)

Figure 4b

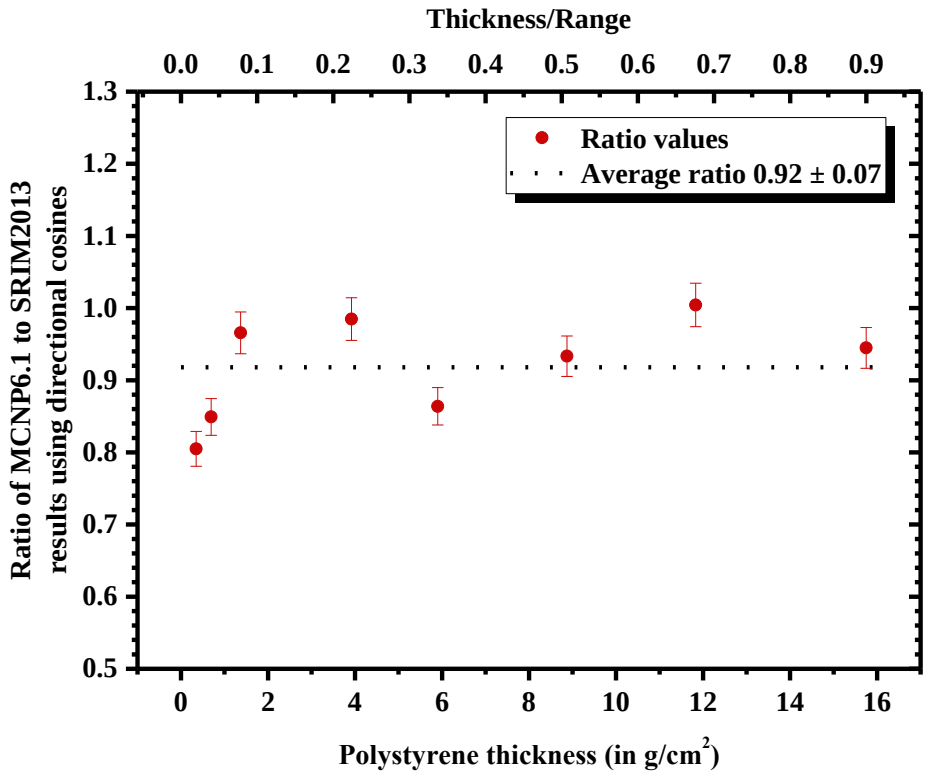
Thickness/Range
0.0
0.1
0.2
0.3
0.4
0.5
0.6
0.7
0.8
0.9
1.3
1.2
1.1
1.0
0.9
0.8
0.7
0.6
0.5
Ratio values
Average ratio 0.92 ± 0.07
Ratio of MCNP6.1 to SRIM2013 results using directional cosines
0
2
4
6
8
10
12
14
16
Polystyrene thickness (in g/cm²)

Figure 4c

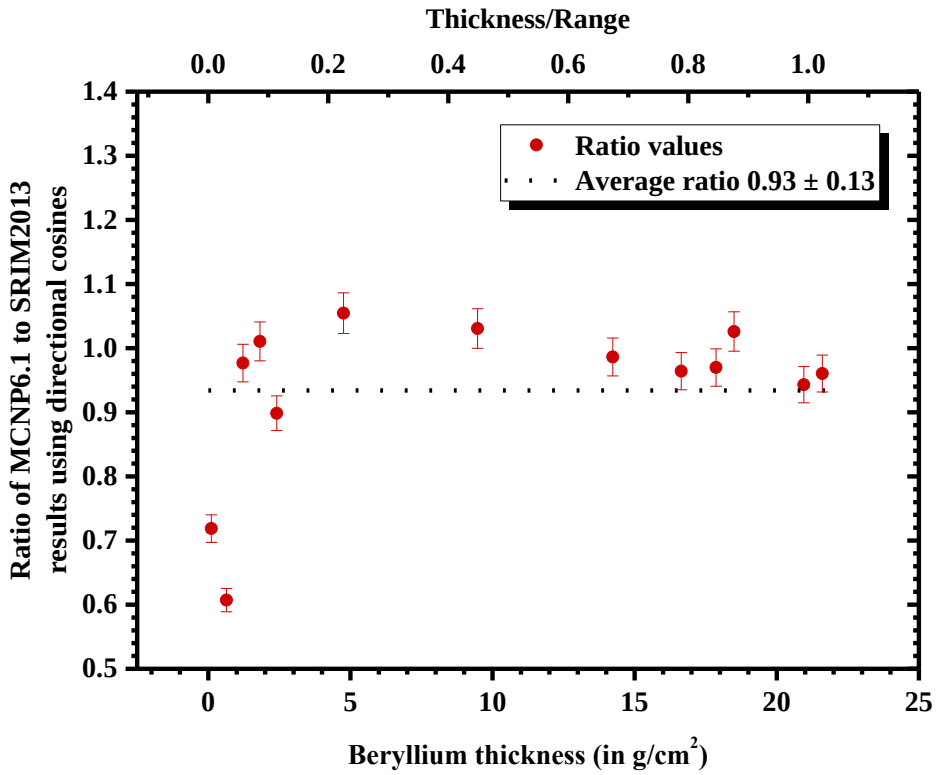
Thickness/Range
0.0
0.2
0.4
0.6
0.8
1.0
1.4
1.3
1.2
1.1
1.0
0.9
0.8
0.7
0.6
0.5
Ratio of MCNP6.1 to SRIM2013 results using directional cosines
Ratio values
Average ratio 0.93 ± 0.13
0
5
10
15
20
25
Beryllium thickness (in g/cm^2)

Figure 4d

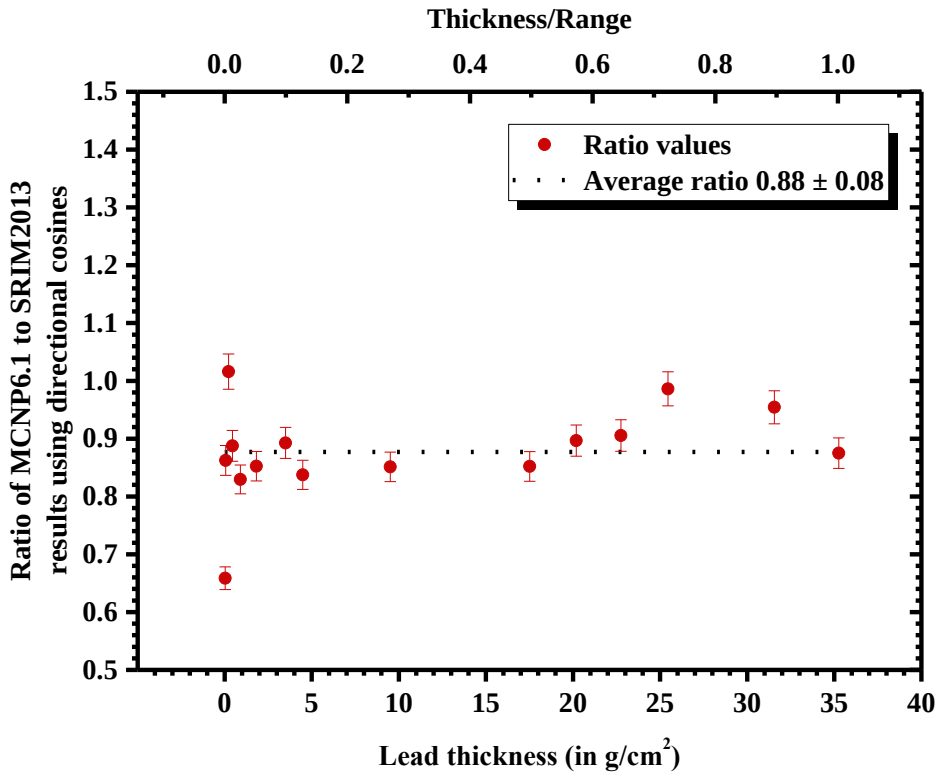
Thickness/Range
0.0
0.2
0.4
0.6
0.8
1.0
1.5
1.4
1.3
1.2
1.1
1.0
0.9
0.8
0.7
0.6
0.5
Ratio of MCNP6.1 to SRIM2013 results using directional cosines
Ratio values
Average ratio 0.88 ± 0.08
0
5
10
15
20
25
30
35
40
Lead thickness (in g/cm2)

Figure 4e